THE JOURNAL OF PHYSICAL CHEMISTRY A

 VOLUME 104, NUMBER 51, DECEMBER 28, 2000

ARTICLES

Electron Paramagnetic Resonance Spectroscopy of Chromium in CrAPO-5 Molecular Sieves

Bohdan V. Padlyak,[†,‡,⊥] Jan Kornatowski,*[,§] Gabriela Zadrozna,[§] Michał Rozwadowski,[||] and Aleksander Gutsze*[,†]

Department of Biophysics, Ludwik Rydygier Medical Academy, 85-067 Bydgoszcz, Poland, Institute of Experimental Physics, University of Gdańsk, 80-952 Gdańsk, Poland, Institute of Chemical Technology II, University of Technology, 85747 München, Germany, and Faculty of Chemistry, Nicholas Copernicus University, 87-100 Toruń, Poland

Received: July 12, 2000; In Final Form: October 6, 2000

A new synthesis strategy with the use of a co-template allowed for the framework substitution of chromium and the preparation of CrAPO-5 with high sorption capacities for nitrogen and benzene (HS samples). For these materials as well as for those synthesized with classical methods and exhibiting low sorption capacities (LS samples), X-band electron paramagnetic resonance (EPR) spectra were measured at room and liquid nitrogen temperatures. The spectra of the as-synthesized HS and LS samples consist of a broad intense line ($g_{eff} = 1.971 \pm 0.001$, $\Delta H_{pp} \cong 500$ G) with a positive lobe at $g_{eff} = 5.15 \pm 0.01$, assigned to the Cr^{3+} ($3d^3$, $^4F_{3/2}$) ions with severely (rhombic) distorted octahedral coordination. The calcined samples show an additional narrow EPR signal of axial symmetry with $g_{||} = 1.971 \pm 0.001$ and $g_{\perp} = 1.959 \pm 0.001$ that is assigned to the Cr^{5+} ($3d^1$, $^2D_{3/2}$) ions in octahedral coordination as well. The HS samples heated under a vacuum exhibit a decrease in intensity of the Cr^{3+} lines as well as several new signals. Two of these signals are characterized by an axially symmetric g factor and belong to the Cr^{5+} centers in square pyramidal and tetrahedral coordinations. The third signal may be assigned to the Cr^{1+} ($3d^5$, $^6S_{5/2}$) ions. The spectra of the LS samples heated under a vacuum show a strong decrease in intensity of the Cr^{3+} lines and only the two signals of the Cr^{5+} centers in the same coordinations. Their g factors are similar to those in the HS samples. The thermal treatments under oxidative (O_2) and reductive (H_2) atmospheres reveal reproducible redox properties of the Cr^{5+} ions and a high stability of the Cr^{3+} ones, especially in the HS samples. The EPR results give strong support for the framework incorporation of the Cr^{3+} ions in the HS materials.

Introduction

Incorporation of transition metals into framework sites of aluminophosphate molecular sieves by isomorphous substitution for Al^{3+} or P^{5+} is a useful tool for the modification of the properties of such materials. However, the transition metals that can easily form ions with various valences and coordination states, e.g., V, Cr, Mo, and W, have generally shown substantial difficulties for incorporation. Chromium belongs to the group of metals that are interesting for catalysis. For example, $AlPO_4$-5 containing Cr has been shown to have potential as a recyclable catalyst for selective oxidation of secondary alcohols to ketones,

[†] Ludwik Rydygier Medical Academy.
[‡] University of Gdańsk.
[§] University of Technology.
[||] Nicholas Copernicus University.
[⊥] On leave from Department of Physics, Ivan Franko National University of Lviv, 50 Dragomanov Street, 79005 Lviv, Ukraine.

10.1021/jp002490n CCC: $19.00
Published on Web 12/05/2000

TABLE 1: Characteristics of the Examined CrAPO-5 Samples (PB = Pseudoboehmite)

sample no	Al compound used for synthesis	Cr/P in reaction gel	Cr content (ICP), mmol/g	uc/Cr	pore volume (BET), cm^3/g
1	PB-like AlO(OH) sol	0.20	0.321	2.0	69
2	PB (Pural)	0.15	0.120	5.5	84
3	amorph $Al(OH)_3$ sol	0.20	0.109	5.5	15
4	amorph $Al(OH)_3$ sol	0.10	0.046	14.0	7

alkylbenzenes to acetophenones, and cyclohexane to cyclohexanone as well as for selective decomposition of cyclohexenyl hydroperoxide to 2-cyclohexen-1-one.[1−4] Therefore, many efforts have been made to incorporate Cr into the frameworks of aluminophosphates, to create isolated redox centers.[1−12] Noteworthy is that the inventors group of all the aluminophosphate molecular sieves, Union Carbide/UOP, called CrAPO-5 material CAPO-5.

Reports on the possible introduction of Cr into silicate molecular sieves have been published more often than those dealing with aluminophosphates. Some authors postulated isomorphous substitution of Cr into framework positions of silicate zeolites. Weckhuysen and Schoonheydt[5,6] reported on electron paramagnetic resonance (EPR) and diffuse-reflectance UV−vis spectroscopy studies of Cr in $AlPO_4$-5 and in various silicates. They concluded that the Cr cannot be substituted into the framework positions but is anchored at the surface, and that this is due mainly to a strong preference of the Cr^{3+} ions for octahedral coordination. Sheldon et al.[1−4] postulated framework substitution of both Cr^{3+} and Cr^{6+} ions in octahedral and tetrahedral coordinations on the basis of catalytic behavior, although Cr^{6+} species could easily be washed out of their calcined materials. Radaev et al.[7] and Thiele et al.[8] investigated large crystals of CrAPO-5 synthesized with the fluoride method and concluded that Cr occurs as an extraframework species. A spectroscopic study[9] of Cr-containing SAPO-5 showed pseudo-octahedrally coordinated Cr^{3+} ions. On the basis of the EPR, electron spin−echo modulation, and UV−vis spectroscopy investigations of CrAPSO-11, Kevan et al.[10] postulated that small amounts of Cr^{3+} can be incorporated into the initial as-prepared materials and that after calcination, chromium is transformed into Cr^{5+} located in the P^{5+} framework sites. The same authors maintained that they evidenced the framework substitution of small amounts of Cr^{3+} and Cr^{5+} ions in CrAPSO-5, from similar EPR and electron spin−echo modulation investigations.[11]

Our synthesis method[12] is the first to allow for the stable substitution of larger amounts of Cr^{3+} for Al^{3+} into the framework of $AlPO_4$-5, i.e., for producing the CrAPO-5 material with high sorption properties typical for AFI (AlPO-Five) structure type (HS samples). Other synthesis procedures, similar to those reported in the above-cited literature, have regularly yielded materials of low or very low sorption properties (LS samples), although most of the other features were similar for both groups.[12,13] Although the applied characterization methods, especially UV−vis spectroscopy, seemed to indicate the framework incorporation of chromium,[12,13] the final determination of valence state(s) and geometry of local environment(s) of the Cr ions in both types of the CrAPO-5 materials appeared to be difficult. Therefore, we performed detailed EPR examinations to study the features, local symmetry, and stability of chromium in the $AlPO_4$-5 structure as well as the behavior of the incorporated Cr ions during thermal treatment under oxidative (O_2) and reductive (H_2) atmospheres.

Experimental Section

Preparation of CrAPO-5. The CrAPO-5 samples were synthesized following the general procedure for growing large crystals,[14−16] modified by the use of co-template(s) and appropriate Al compounds as described elsewhere.[12,13] The reaction gels had molar ratios of the components as oxides: a Al_2O_3: b P_2O_5: c Cr_2O_3: d R: e H_2O, where R is triethylamine; a = 0.80−1.0, b = 1.0−1.1, c = 0.05−0.3, d = 1.25−1.65, e = 200−350. Several Al compounds were used: crystalline hydroxides with the pseudoboehmite structure (Pural SB and Catapal Vista), pseudoboehmite-like Al oxide hydrate sol,[14−16] and noncrystalline compounds Al hydroxide sol and Al isopropoxide. The reaction gels were treated hydrothermally in Teflon-lined autoclaves at 463 K for 2 to 5 days. The products were calcined under a slow stream of air at 773 K for at least 48 h. More details are given in refs 12 and 13.

Redox treatments of the samples were performed in special Varian tubes with the use of the Balzers-Pfeifer vacuum system, high-purity oxygen or hydrogen, and an automatic electric furnace controlled by a computer. The processes were performed by heating the samples to 773 K and exposing them to an oxygen or hydrogen atmosphere (10 mbar) at that temperature for 12 h.

EPR Measurements. X-band EPR spectra of the CrAPO-5 samples were measured at room and liquid nitrogen temperatures using a RADIOPAN SE/X-2544 commercial spectrometer with an RCX 660 cylindrical TM_{110} cavity, operating in the high-frequency (100 kHz) modulation mode of the magnetic field. The EPR spectra were measured on the polycrystalline CrAPO-5 samples, closed under air and a vacuum in high-purity quartz tubes from Varian.

The g-values of the EPR lines were determined from the experimental spectra using the resonance relationships and the BRUKER computer simulation program "SimFonia". The microwave frequency in each specific case was determined by means of a polycrystalline diphenylpicrylhydrazyl (DPPH) frequency marker (g = 2.0036 ± 0.0001) and the EPR line of the coke radicals (g = 2.0032 ± 0.0001).

To compare the results with known data, we measured a simple model system, Cr/Al_2O_3, after pretreatments similar to those used in the CrAPO-5 samples.

Results and Discussion

Characteristics of the CrAPO-5 Materials. The CrAPO-5 crystals had dimensions within the range of 20 to 80 μm and a morphology of single hexagonal prisms, typical of the AFI structure type.[12,13] All the CrAPO-5 samples had an intense green color after synthesis.[12,13] After calcination and removal of the template, the samples synthesized from the pseudoboehmite Al compounds were colored yellow-green (samples 1 and 2, Table 1). Color of the other samples (from amorphous Al compounds) ranged from greenish-gray to dirty gray (samples 3 and 4, Table 1).[12,13] The yellow-green color of samples 1 and 2 could change to violet and back to yellow-green, depending on the state of hydration,[13] whereas the gray color of samples 3 and 4 was stable and independent of any treatment. These changes were reflected in the UV−vis spectra corresponding to the different local environment of chromium in the samples.[13]

The yellow-green samples showed an adsorption capacity for water that is typical of the AFI structure type, as well as a high

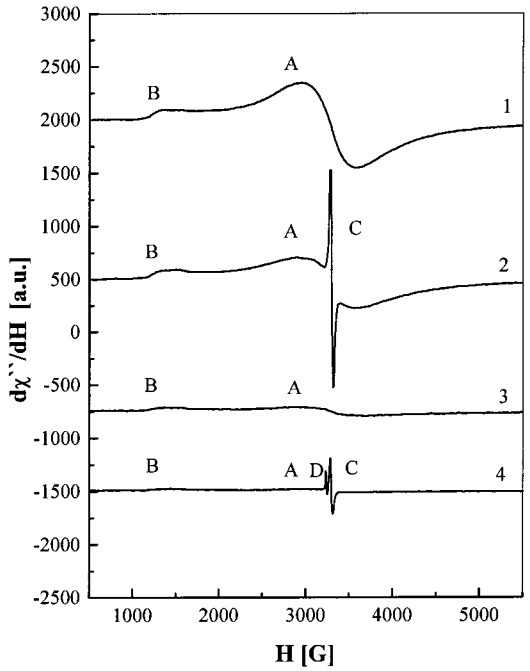

Figure 1. Typical complete EPR spectra recorded at 300 K for the HS (1, 2) and LS (3, 4) CrAPO-5 samples 1 and 3 (Table 1): 1, 3—as-synthesized; 2, 4—calcined. The spectra of samples 2 and 4 (Table 1) are identical with those shown here.

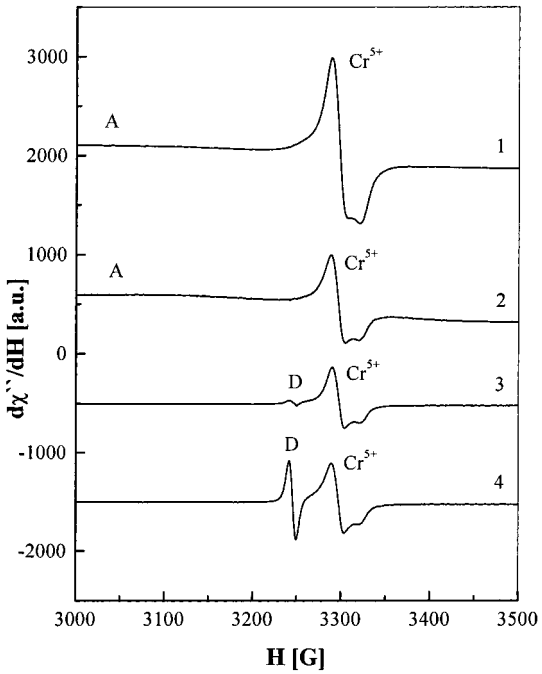

Figure 2. Central region of EPR spectra recorded at 300 K for the HS (1, 2) and LS (3, 4) CrAPO-5 samples calcined at 773 K.

adsorption capacity for benzene and nitrogen (HS, high sorption samples 1 and 2).[12,13] The gray samples hardly adsorbed nitrogen or benzene, and their sorption of water was also somewhat reduced (LS, low sorption samples 3 and 4).[12,13] This behavior indicated an open state of the channels in the HS materials and clogged channels in the LS ones.

EPR Spectra of As-Synthesized and Calcined CrAPO-5. The typical X-band EPR spectra measured at 300 K for the as-synthesized HS (Figure 1, spectrum 1) and LS samples (spectrum 3) were similar. The spectra measured at liquid nitrogen temperature were similar as well. The spectra consisted of a broad line A ($g_{eff} = 1.971 \pm 0.001$, $H_{pp} \cong 500$ G) of Lorenz shape with a positive lobe B ($g_{eff} = 5.15 \pm 0.01$). The intensities of the A and B lines varied strongly between the samples (Figure 1). Similar EPR spectra have been observed for Cr in alumina,[17] silica,[18] chromosilicate,[19] molecular sieves of AEL[10,20] and AFI types,[11] and a number of other compounds with a disordered structure, particularly in the Cr-doped glasses of different compositions.[21−23] Both observed signals have been assigned to the Cr^{3+} ($3d^3$, $^4F_{3/2}$) ions. The A and B lines were originally interpreted[18] using analysis of the spin Hamiltonian:

$$H = \beta \mathbf{H}\cdot g\cdot \mathbf{S} + D[S_z^2 - 1/3S(S+1)] + E(S_x^2 - S_y^2) \quad (1)$$

where D and E are the axial and orthorhombic crystal field terms, respectively. Such interpretation of the EPR spectra of the Cr^{3+} ions in disordered systems has been confirmed in several studies[11,20−23] and supported for CrAPSO-5 on the basis of computer simulation.[11] In particular, the best fit has been obtained for the following parameters of the spin Hamiltonian: $g_\perp = 1.98$, $g_\parallel = 1.80$, $D = 0.50$ cm^{-1}; $E/D = 1/3$, and peak-to-peak line width $\Delta H_{pp} = 300$ G. The simulated EPR spectrum of the Cr^{3+} ions showed a weak line at $g_3 = 0.98$ in addition to the two well-known lines at $g_1 = 5.20$ and $g_2 = 2.00$. This weak line was found in the experimental spectra of CrAPSO-5,[11] whereas in the EPR spectra of our CrAPO-5, samples this line was not observed.

Significant broadening of the EPR lines of Cr^{3+} in our CrAPO-5 samples ($\Delta H_{pp} \cong 500$ G) in relation to the same lines for the CrAPSO-5 materials with very low Cr content[11] ($\Delta H_{pp} = 300$ G) might be related to a dipolar interaction of the Cr^{3+} ions.[23−25] Similar EPR spectra have also been observed for the isolated and dipolar-coupled Cr^{3+} ions in the Cr/Al_2O_3 preparation used as a model system in our investigations.

On the basis of comparison of our experimental data with those reported in the cited literature,[17−23] the observed EPR spectra of the as-synthesized HS and LS samples can be assigned to the Cr^{3+} ions in the sites with strongly rhombic distorted ($|E/D| = 1/3$) octahedral coordination. Therefore, we may assume that the chromium ions occur in the CrAPO-5 framework mainly as $CrO_{4/2}^-$ units, complemented by two H_2O molecules from the pores to achieve a distorted octahedral coordination. This coordination gives the intense green color of the species which replace $AlO_{4/2}^-$ tetrahedra in the framework.[12,13] The EPR lines of Cr^{3+} are much more intense (over 10 times more) for the HS samples than for the LS ones (Figure 1), despite much smaller differences in Cr contents of the crystals (Table 1). The differences in intensities suggest that some part of the chromium may be retained during the synthesis as ions of a higher valence that may also be attached to the framework. This correlates with the UV−vis spectroscopy data which show, in addition to the strong bands at about 625, 445, and 290 nm assigned to the octahedrally coordinated Cr^{3+} ions, weaker bands at about 280 and 330−350 nm corresponding to the ($O \rightarrow Cr^{6+}$) and/or ($O \rightarrow Cr^{5+}$) charge-transfer transitions.[13] As can be concluded from the UV−vis spectra, the LS samples have a higher content of Cr^{6+}/Cr^{5+} and a lower content of Cr^{3+} than do the HS samples. It should be noted that the concentration of the Cr^{5+} ions in the as-synthesized HS and LS samples is negligible and that their EPR spectra were not observed. Therefore, the Cr^{6+} ions are the higher-valence form of chromium occurring in the as-synthesized CrAPO-5 samples, and they should be attached to the framework.

EPR spectra of the calcined HS and LS samples showed a new narrow signal of chromium, denoted as C (Figure 1, spectra 2, 4). The C signals were identical for all calcined HS and LS

TABLE 2: The *g* Factors for the Signals C of the Calcined CrAPO-5 Samples Obtained as the Best Fit of the Experimental (T = 300 K) and Simulated EPR Spectra

		HS sample		LS sample		
Cr ion	*g* factor	1	2	3	4	notes
Cr^{5+}	g_{xx}	1.970 ± 0.001	1.971 ± 0.001	1.972 ± 0.001	1.972 ± 0.001	$g_{xx} = g_{yy} =$
	g_{yy}	1.970 ± 0.001	1.971 ± 0.001	1.972 ± 0.001	1.972 ± 0.001	$= g_{\perp}$
	g_{zz}	1.959 ± 0.001	1.959 ± 0.001	1.959 ± 0.001	1.959 ± 0.001	$g_{zz} = g_{\parallel}$

samples and consist of two weakly resolved lines (Figure 2, spectra 1−4), which were not better resolved at liquid nitrogen temperature. However, the spectra of the calcined LS samples showed an additional isotropic symmetrical line D with g = 2.0032 ± 0.0001 and ΔH_{pp} = 7.5 ± 1.0 G (Figure 1, spectrum 4 and Figure 2, spectra 3, 4). This D line was assigned to coke radicals[26] which were formed in the channels from the organic template molecules during the calcination process. A small amount of coke present in the LS samples could provide an internal reference for determination of the *g*-values.

The parameters obtained from the experimental spectra have offered a possibility to simulate the C signal observed in calcined samples (Figure 2, spectra 1−4). The computer simulation was performed with the use of standard methods for disordered (polycrystalline or powdered) samples. The most suitable line width and line shape were selected, and the best fit of the simulated spectra to the experimental ones was obtained assuming the Lorenz line shape with ΔH_{pp} = 16.5 ± 1.0 G. The corresponding *g* factor values are given in Table 2.

The *g* factors obtained for the C signals of all calcined HS and LS samples (Table 2) are similar to those of the octahedrally coordinated Cr^{5+} ions in silica−alumina and alumina.[17,27−30] It should be noted that EPR spectra of Cr^{5+} in silica−alumina with low Al_2O_3 content (3 wt %) are characterized by anisotropic *g* factors and line widths similar to those in Cr/SiO_2 ($g_{\perp} = 1.98$, $g_{\parallel} = 1.90$, ΔH_{pp} = 15 G). An increase in the Al_2O_3 content to 10 wt % leads to a change in the spectral parameters of Cr^{5+} ($g_{\perp} = 1.97$, $g_{\parallel} = 1.95$, ΔH_{pp} = 20 G). In the result, the Cr/Al_2O_3 system is characterized by an isotropic symmetric line with $g_0 = 1.96$ and ΔH_{pp} = 44 G. The isotropic symmetric EPR line of the Cr^{5+} ions with $g_0 = 1.972 \pm 0.001$ and ΔH_{pp} = 47.0 ± 1.0 G has also been observed by us in the Cr/Al_2O_3 model system calcined in air at 700 K. These changes of the EPR spectra are caused by the transformation of the coordination of Cr^{5+} from tetrahedral (local symmetry—T_d) in SiO_2 to square pyramidal with a short chromyl bond (local symmetry—C_{4v}) in Al_2O_3.[27,30] Adsorption of H_2O results in the transformation of the tetrahedral and square-pyramidal coordinations of Cr^{5+} to an octahedral one in Cr/SiO_2, $Cr/SiO_2-Al_2O_3$, and Cr/Al_2O_3 systems and leads to an increase of the $g_{\parallel}$-value from 1.90 to 1.95, i.e., to "symmetrization" of the EPR spectra.[31,32] Similar anisotropic EPR signals, with $g_{\perp} = 1.97$, $g_{\parallel} = 1.95$, of the octahedrally coordinated Cr^{5+} ions have been observed in the hydrated ZSM-5-type zeolites.[33,34] During an oxidation process, the Cr^{5+} ions are stabilized in the channels of ZSM-5 as CrO_2^+ particles with a part of nonframework O^{2-} ligands.[33,34] These isolated ions in the zeolite structure may be considered as coordinatively nonsaturated surface ions which define catalytic activity of the material.[34]

Therefore, the C signal was identified as corresponding to the isolated Cr^{5+} ions in axially distorted octahedral sites. This signal appears after the calcination process and indicates that a certain part of the Cr^{3+} ions is oxidized to Cr^{5+} in the sites with a more symmetric, octahedral coordination.

The UV−vis spectra of the calcined HS samples showed no shift of the Cr^{3+} d−d bands and a small increase of the Cr^{6+} charge-transfer bands. These facts confirm that a certain part of the Cr^{3+} ions is oxidized to the Cr^{5+} and Cr^{6+} states, as is

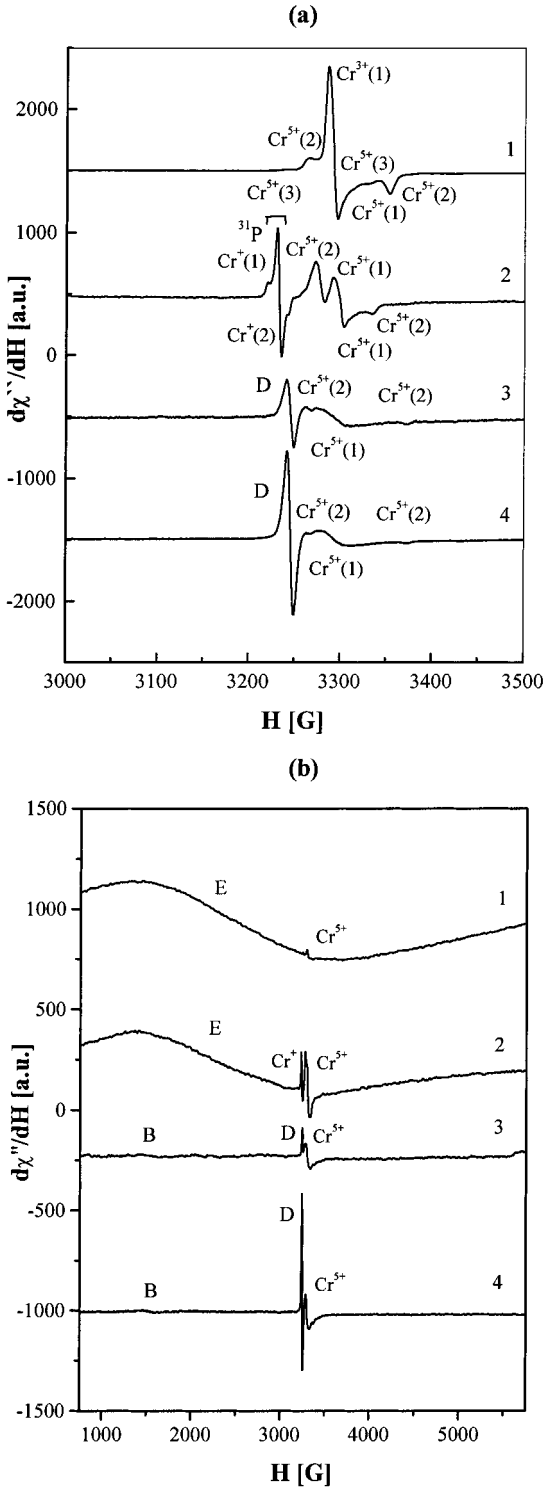

Figure 3. EPR spectra (300 K) of the HS (1, 2) and LS (3, 4) CrAPO-5 samples after heating at 773 K under vacuum (2×10^{-7} mbar) for 12 h: (a) complete and (b) central region of spectra.

TABLE 3: Assignments and *g* Factors of the Experimental EPR Signals ($T = 300$ K) of Chromium Ions in the CrAPO-5 Samples after Heating at 773 K under a Vacuum (2×10^{-7} mbar) for 12 h, and Corresponding Coordination of the Cr Centers

		HS sample		LS sample		
Cr ion	*g* factor	1	2	3	4	coordination
Cr^{5+} (1)	$g_{\|\|}$	1.962 ± 0.001	1.960 ± 0.001	1.962 ± 0.002	1.961 ± 0.002	square-
	$g_{\perp}$	1.974 ± 0.001	1.969 ± 0.001	1.975 ± 0.002	1.974 ± 0.002	pyramidal
Cr^{5+} (2)	$g_{\|\|}$	1.943 ± 0.002	1.951 ± 0.002	1.930 ± 0.002	1.930 ± 0.002	tetrahedral
	$g_{\perp}$	1.990 ± 0.002	1.982 ± 0.002	1.991 ± 0.002	1.991 ± 0.002	
Cr^{5+} (3)	$g_{\|\|}$	1.951 ± 0.002	not observed	not observed	not observed	tetrahedral
	$g_{\perp}$	1.999 ± 0.002				
Cr^{1+} (1)	g_{iso}	not observed	2.005 ± 0.001	not observed	not observed	near to P^{5+} ion
Cr^{1+} (2)	g_{iso}	not observed	2.005 ± 0.001	not observed	not observed	unknown

reflected in a partial change in the color of the sample, to yellow. The charge-transfer band of Cr^{6+} for the calcined LS samples is stronger than that in the HS ones.[13] These results correlate with the present EPR data showing more intense signals of Cr^{3+} for the HS than for the LS samples (Figures 1, 2).

EPR Spectra of CrAPO-5 Heated Under a Vacuum. Heat treatment of the calcined HS samples at 773 K under a vacuum (2.4×10^{-7} mbar) for 12 h led to dehydration and lowering of the coordination of the chromium ions. In the result, the lines of Cr^{3+} (A and B lines in Figure 1) and Cr^{5+} (C line in Figure 2) vanished and several new signals of chromium appeared (Figure 3). Instead of the former Cr^{3+} signals, a new, extremely broad ($\Delta H_{pp} \cong 2500$ G) and intense signal with $g = 2.55 \pm 0.01$ appeared, which was also attributed to Cr^{3+} (Figure 3a, line E). A similar EPR line of the Cr^{3+} ions was observed earlier in CrAPSO-11 and CrAPSO-5 molecular sieves,[10,11] chromia-alumina,[17] and Cr-containing phosphate glasses due to a dipolar broadening.[23,25] A similar signal was also recorded for dipolar- and exchange-coupled pairs of the Cr^{3+} ions individually six-coordinated in the structure of the α-Cr_2O_3 antiferromagnetic phase.[24] For our HS samples, with their high sorption capacities, such interpretation is excluded. A further study of the nature of the Cr^{3+} broad signal with $g = 2.55 \pm 0.01$ is necessary.

The new narrow lines were three EPR signals of the Cr^{5+} centers for the dehydrated HS (1) sample as well as two signals of the Cr^{5+} and two signals of the Cr^{1+} centers of the dehydrated HS (2) sample (Figure 3b, spectra 1, 2). Identification of the observed new chromium centers was made on the basis of literature data for other Cr-containing zeolitic and oxidic compounds such as silica, silica−alumina, and alumina.[10,11,27−34] Assignments, *g* factors, and possible coordinations of chromium centers for all investigated samples after such treatment are presented in Table 3.

EPR signals of the Cr^{5+} ($3d^1$, $^2D_{3/2}$) ions in the dehydrated HS (1) sample are characterized by axially symmetric *g* factors and belong to the centers in square-pyramidal {Cr^{5+} (1) lines} and tetrahedral {Cr^{5+} (2) and Cr^{5+} (3) lines} coordinations. The axially symmetric EPR signals of the HS (2) sample similarly belong to Cr^{5+} (1) and Cr^{5+} (2) centers in the square-pyramidal and tetrahedral coordinations, respectively. The EPR signal of the Cr^{1+} ($3d^5$, $^6S_{5/2}$) ions, consisting of one narrow ($\Delta H_{pp} \cong 9$ G) line (for Cr^{1+} (2) centers) and two symmetric satellites {for Cr^{1+} (1) centers}, is characterized by an isotropic *g* factor ($g_{iso} = 2.005 \pm 0.001$). In our opinion, the two satellite lines are caused by superhyperfine (SHF) interaction (isotropic SHF constant $a_{iso} \cong 21$ G) of the Cr^{1+} (1) centers with one nucleus of the ^{31}P isotope (nuclear spin $I = 1/2$, natural abundance 100%).

Vacuum heat treatment of the calcined LS samples under the same conditions as for the HS samples led to a strong decrease of the Cr^{3+} centers (A and B lines in Figure 1) and full disappearance of the octahedral Cr^{5+} ones (signal C in Figure 2). Instead of the former Cr^{5+} signals, two new EPR signals appeared which were attributed to the Cr^{5+} (1) and Cr^{5+} (2) centers with square-pyramidal and tetrahedral coordinations, respectively (Figure 3, spectra 3, 4) and with the *g* factors similar to those of the HS samples (Table 3). Only traces of the A and B signals of Cr^{3+} (Figure 3a, spectra 3, 4) were observed for the LS samples after vacuum heat treatment, whereas the broad Cr^{3+} signal with $g = 2.55 \pm 0.01$ (line E) was not observed. Together with the gray color, these spectral features indicated that only a small amount of the Cr^{3+} ions could be substituted into the framework positions of the LS samples.

The observed new forms of the Cr^{5+} and Cr^{1+} centers might be created from the extraframework (or surface) Cr^{6+} and Cr^{2+} ions, respectively, under the vacuum heat treatment. A type of disproportionation reaction of the Cr^{5+} or/and Cr^{3+} ions might also be imagined.

Redox Behavior of the CrAPO-5 Samples. Stability of the observed Cr^{1+}, Cr^{3+}, and Cr^{5+} ions in CrAPO-5 was studied by applying redox processes to the calcined HS and LS samples, pretreated in a vacuum. The heat treatments in the oxidative and reductive atmospheres did not considerably affect the Cr^{3+} ions in either the HS or the LS materials, but strongly influenced the Cr^{1+} and Cr^{5+} centers.

Figure 4 shows changes in the EPR spectra of the sample HS (2) after various oxidative and reductive treatments. It should be noted that the spectra of the Cr^{1+} centers were unstable and that their intensities decreased strongly after exposure to air at room temperature, whereas the intensities of the spectra of the Cr^{5+} (1) and Cr^{5+} (2) centers were only slightly reduced under the same conditions (Figure 4a, spectra 1, 2). Adsorption of O_2 at 300 K with further evacuation of residual gas led to an increase in the intensity of the Cr^{1+} lines and an improvement in the resolution of the Cr^{5+} (1) and Cr^{5+} (2) lines (Figure 4a, spectrum 3). The observed differences between exposure to air and pure O_2 at room temperature may be connected with the adsorption of water from the air, i.e., hydration of the sample.

Heat treatment at 573 K in a vacuum led to a decrease in intensity of the Cr^{1+} and to an increase in intensity of the Cr^{5+} (1) and Cr^{5+} (2) EPR signals. This heat treatment also led to an appearance of the additional signal of Cr^{5+} (3) (Figure 4a, spectrum 4) with *g* factors $g_{||} = 1.951 \pm 0.002$ and $g_{\perp} = 1.999 \pm 0.002$, similar to those of the Cr^{5+} (3) signal for the vacuum-pretreated HS (1) sample (Table 3). Oxidation of the HS (2) sample in an O_2 atmosphere at 773 K led to full disappearance of the EPR lines of Cr^{1+} and an appearance of a complex spectrum (Figure 4b, spectrum 5), similar to that for the HS (1) sample pretreated in a vacuum (Figure 3b, spectrum 1). This complex spectrum belongs to the Cr^{5+} (1), Cr^{5+} (2), and Cr^{5+} (3) centers, which are characterized by axially symmetric *g* factors similar to those for the same Cr^{5+} centers in the HS (1) sample (Table 3). The reduction of the HS (2) sample with hydrogen at 773 K led to full disappearance of all EPR lines

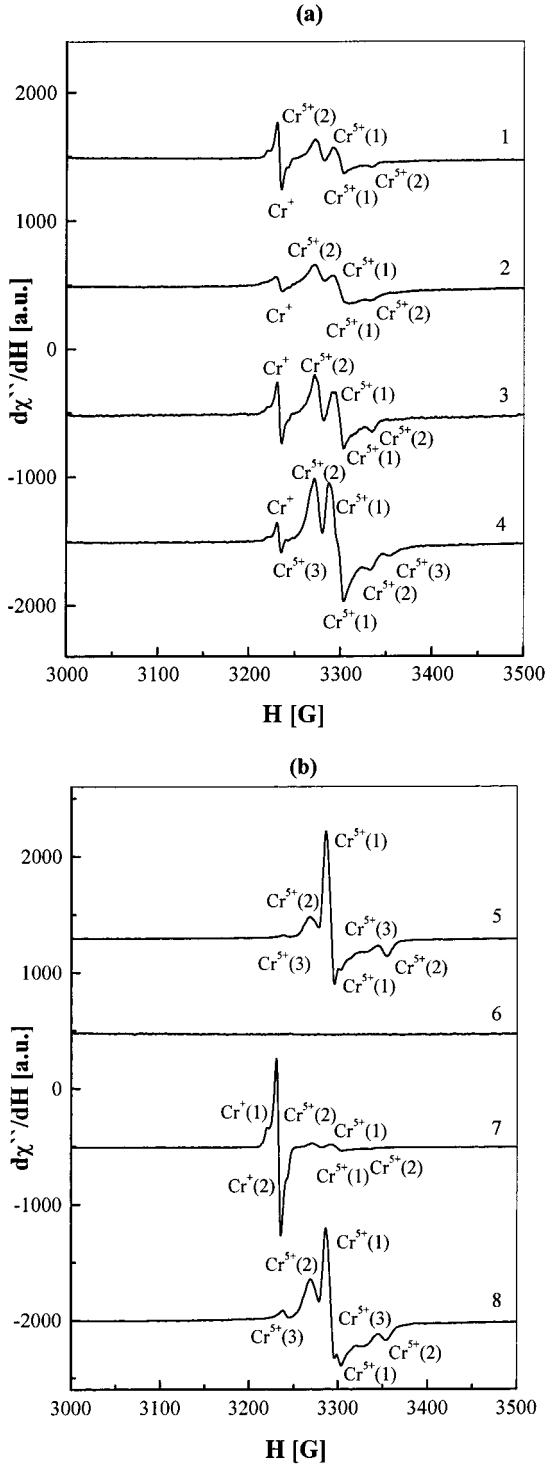

Figure 4. Central region of EPR spectra recorded at 300 K for the calcined HS (2) sample after the following treatments: (a) heating at 773 K under a vacuum (2×10^{-7} mbar) for 12 h (1), exposure to air (10 mbar) at 300 K for 85 h (2), adsorption of O_2 (10 mbar) at 300 K and evacuation (3), heating at 573 K under vacuum (8.9×10^{-6} mbar) for 1 h (4); (b) heating at 773 K in O_2 (10 mbar) for 12 h and evacuation (5), heating at 773 K in H_2 (10 mbar) for 12 h and evacuation (6), exposure to air (10 mbar) for 4 h (7), heating at 773 K in O_2 (10 mbar) for 12 h and evacuation (8).

(Figure 4b, spectrum 6). Exposure to air at 300 K restored the initial Cr^{1+} and Cr^{5+} EPR spectra (Figure 4b, spectrum 7). Reoxidation in the O_2 atmosphere at 773 K led to full disappearance of the Cr^{1+} spectra and restored the well-resolved complex EPR spectrum (Figure 4b, spectrum 8), similar to that

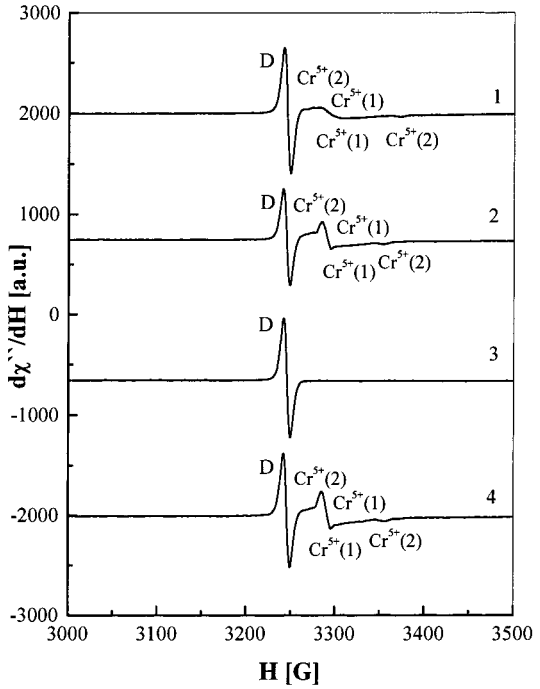

Figure 5. Central region of EPR spectra (300 K) of the calcined LS (4) sample after heating at 773 K for 12 h: (1) under a vacuum (2×10^{-7} mbar), (2, 4) in oxidizing atmosphere (O_2, 10 mbar), and (3) in reducing (H_2, 10 mbar) atmosphere.

of the HS (1) sample (Figure 3b, spectrum 1) and the HS (2) sample after the first oxidation (Figure 4b, spectrum 5).

The LS samples of CrAPO-5 revealed redox properties similar to those of the HS samples. Figure 5 shows the changes in EPR spectra of the LS (4) sample calcined and pretreated in a vacuum (spectrum 1); after oxidation in oxygen (spectra 2, 4); and after reduction in hydrogen (spectrum 3). Oxidation of the LS (4) sample led to an insignificant change in the line width of Cr^{5+} (1) centers and the $g_{||}$ value of Cr^{5+} (2) centers (Figure 5, spectrum 2). The hydrogen reduction of the LS (4) sample led to a full disappearance of the lines of the Cr^{5+} (1) and Cr^{5+} (2) centers (Figure 5, spectrum 3). Reoxidation in oxygen gave the same EPR spectra of the Cr^{5+} (1) and Cr^{5+} (2) centers, as after the first oxidation (Figure 5, spectrum 4). A decrease of the line width of Cr^{5+} (1) centers and anisotropy of the g factor of the Cr^{5+} (2) centers in the LS (4) sample after oxidation might suggest a partial healing of the structure under the oxidative treatment,[35] in the sense of incorporation of chromium into the framework positions. However, the almost constant line intensity of the coke radicals (Figure 5, line D) observed for the LS (4) sample during the redox processes indicated that a considerable part of chromium was still remaining as an extraframework species in the channels; this part made the complete removal of organic carbonaceous residuals impossible.

Conclusions

Cr in the HS samples occurs mostly as Cr^{3+} in octahedral form $[CrO_{4/2}L_2]^-$ as a framework species. A certain amount of Cr^{6+} and/or Cr^{5+}, seen with UV−vis and/or EPR spectroscopy, seems to be either a framework species substituted for P or, more likely, a type of surface species anchored to the framework and not hindering diffusion and sorption in the channels. In the LS samples, the Cr^{6+} and/or Cr^{5+} are present to a distinctly higher extent, which most likely results in the clogging of the pores.

In the vacuum-pretreated calcined HS materials, Cr remains mostly as Cr^{3+}, and two forms of Cr^{5+} appear: square-pyramidal

(five coordinated) chromyl groups and tetrahedrally coordinated Cr^{5+} centers. The latter may be an extraframework species. In the vacuum-pretreated calcined LS materials, mainly tetrahedral extraframework Cr^{5+} species occur, and Cr^{3+} exists in small amounts only. The LS samples also show a strong signal from carbon that is extremely resistant to oxidation. Thus, the vacuum heat treatment of the calcined samples confirms the occurrence of Cr^{3+} in strongly prevailing amounts in the HS materials and indicates that only small amounts of Cr^{3+} exist in the LS ones. Formation of a small amount of Cr^{5+}, which does not hinder adsorption in the HS samples, may suggest that these ions might be substituted for P.

Oxidative and reductive treatments reveal reproducible redox properties of the Cr^{5+} ions in square-pyramidal and tetrahedral coordinations, in both the HS and the LS calcined and vacuum-pretreated CrAPO-5 samples. These treatments do not considerably influence the EPR spectra of the Cr^{3+} ions in these CrAPO-5 samples. The results reveal a high stability of the Cr^{3+} ions, especially in the HS CrAPO-5 materials, that can be justified only by framework incorporation.

In general, the EPR investigation gave strong support for the results, reported separately,[12,13] that have been obtained with many other, also spectroscopic characterization methods. This outcome allowed for the conclusion that the new synthesis procedure yields the AFI-type materials with chromium stably incorporated into the framework positions.

Acknowledgment. The work was partially supported by the University of Gdańsk within Grant No. BW5200-5-0304-0, by the Deutsche Forschungsgemeinschaft, and by the Polish Committee for Scientific Research (KBN) within Grant No. 3T09A04714.

References and Notes

(1) (a) Chen, J. D.; Haanepen, M. J.; Van Hooff, J. H. C.; Sheldon, R. A. *Stud. Surf. Sci. Catal.* **1994**, *84*, 973. (b) Chen, J. D.; Dakka, J.; Neeleman, E.; Sheldon, R. A. *J. Chem. Soc., Chem. Commun.* **1993**, 1379.

(2) Lempers, H. E. B.; Sheldon, R. A. *Stud. Surf. Sci. Catal*. **1997**, *105*, 1061.

(3) Lempers, H. E. B.; Chen, J. D.; Sheldon, R. A. *Stud. Surf. Sci. Catal*. **1995**, *94*, 705.

(4) Sheldon, R. A.; Chen, J. D.; Dakka, J.; Neeleman, E. *Stud. Surf. Sci. Catal*. **1994**, *83*, 407.

(5) Weckhuysen, B. M.; Schoonheydt, R. A. *Zeolites* **1994**, *14*, 360.

(6) Weckhuysen, B. M.; Schoonheydt, R. A. *Stud. Surf. Sci. Catal*. **1994**, *84*, 965.

(7) Radaev, S. F.; Joswig, W.; Baur, W. H. *J. Mater. Chem.* **1996**, *6*, 1413.

(8) Thiele, S.; Hoffmann, K.; Vetter, R.; Marlow, F.; Radaev, S. *Zeolites* **1997**, *19*, 190.

(9) Demuth, D.; Unger, K. K.; Schüth, F.; Srdanov, V. I.; Stucky, G. D. *J. Phys. Chem.* **1995**, *99*, 479.

(10) Zhu, Z.; Wasowicz, T.; Kevan, L. *J. Phys. Chem.* **1997**, *B101*, 10763.

(11) Zhu, Z.; Kevan, L. *Phys. Chem. Chem. Phys.* **1999**, *1*, 199.

(12) Kornatowski, J.; Zadrozna, G. *Proceedings of the 12th International Zeolite Conference*, Baltimore, MD, 1998; Treacy, M. M. J., Marcus, B. K., Bisher, M. E., Higgins, J. B., Eds.; Materials Research Society: Warrendale, PA, 1999; Vol. III, p 1577.

(13) Kornatowski, J.; Zadrozna, G.; Rozwadowski, M.; Zibrowius, B.; Marlow, F.; Lercher, J. A. *Chem. Mater.*, submitted for publication.

(14) Kornatowski, J.; Finger, G. *Bull. Soc. Chim. Belg.* **1990**, *99*, 857.

(15) Finger, G.; Richter-Mendau, J.; Bülow, M.; Kornatowski, J. *Zeolites* **1991**, *11*, 443.

(16) Kornatowski, J.; Rozwadowski, M.; Finger, G. *Pol. Pats.* PL 166147, 166149, 166162, 166505 (all 1995).

(17) O'Reilly, D. E.; Maclver, D. S. *J. Phys. Chem*. **1962**, *66*, 276.

(18) Cornet, D.; Burwell, R. L. *J. Am. Chem. Soc*. **1968**, *90*, 2489.

(19) Przheval'skaya, L. K.; Shvets, V. A.; Kazanskii, V. B. *Kinet. Katal.* **1970**, *11*, 1085.

(20) Weckhuysen, B. M.; Schoonheydt, R. A.; Mabbs, F. E.; Collison, D. *J. Chem. Soc., Faraday Trans*. **1996**, *92*, 2431.

(21) Zakharov, V. K.; Yudin, D. M. *Sov. Phys. Solid State* **1965**, *7*, 1267.

(22) Padlyak, B. V.; Gutsze, A. *Appl. Magn. Reson.* **1998**, *14*, 59.

(23) Landry, R. J.; Fournier, J. T.; Young, C. G. *J. Chem. Phys.* **1967**, *46*, 1285.

(24) Trounson, E. P.; Bleil, D. F.; Wagness, R. K.; Maxwell, R. L. *Phys. Rev.* **1950**, *79*, 542.

(25) Fournier, J. T.; Landry, R. J. *J. Chem. Phys.* **1971**, *55*, 2522.

(26) Lange, J.-P.; Gutsze, A.; Karge, H. G. *J. Catal.* **1988**, *114*, 136.

(27) Van Reijen, L. L.; Cossee, P.; Haren, H. J. *J. Chem. Phys.* **1963**, *38*, 572.

(28) Pecherskaya, Yu. N.; Kazanskii, V. B. *Kompleksoobrazovanie v Katalize (Formation of Complexes in Catalysis)*; Nauka: Moscow, 1968.

(29) Boreskov, G. K.; Bukanaeva, F. M.; Dzisko, V. A. *Kinet. Katal.* **1964**, *5*, 434.

(30) Van Reijen, L. L.; Cossee, P. *Discuss. Faraday Soc*. **1966**, *41*, 277.

(31) Kazanskii, V. B.; Pecherskaya, Yu. N. *Kinet. Katal.* **1963**, *4*, 244.

(32) Kucherov, A. V.; Slinkin, A. A. *Zeolites* **1987**, *7*, 38 and 43.

(33) Kucherov, A. V.; Slinkin, A. A. *Kinet. Katal.* **1986**, *27*, 1199.

(34) Slinkin, A. A.; Kucherov, A. V.; Goryaschenko, S. S.; Aleshin, E. G.; Slovetskaya, K. I. *Kinet. Katal.* **1986**, *30*, 184.

(35) Brückner, A.; Lohse, U.; Mehner, H. *Magnetic Resonance and Related Phenomena*; Ziessow, D., Lubitz, W., Lendzian, F., Eds.; Technische Universität Berlin: Berlin, 1998; Vol. II, p 1053.